

Supplementary Materials for

Inhibition of the Cardiomyocyte-Specific Kinase TNNI3K Limits Oxidative Stress, Injury, and Adverse Remodeling in the Ischemic Heart

Ronald J. Vagnozzi, Gregory J. Gatto Jr., Lara S. Kallander, Nicholas E. Hoffman, Karthik Mallilankaraman, Victoria L. T. Ballard, Brian G. Lawhorn, Patrick Stoy, Joanne Philp, Alan P. Graves, Yoshiro Naito, John J. Lepore, Erhe Gao, Muniswamy Madesh, Thomas Force*

*Corresponding author. E-mail: thomas.force@temple.edu

Published 16 October 2013, *Sci. Transl. Med.* **5**, 207ra141 (2013)
DOI: 10.1126/scitranslmed.3006479

The PDF file includes:

Methods

Fig. S1. TNNI3K is localized to the cardiomyocyte nucleus.

Fig. S2. Basal LV function, hemodynamics, and cardiac morphometry in Tg-TNNI3K and Tg-KI TNNI3K mice.

Fig. S3. Post-I/R activation status of ERK1/2, JNK, and Akt in TNNI3K transgenic mice.

Fig. S4. Basal p38 MAPK activation status in TNNI3K transgenic mice.

Fig. S5. ERK1/2, JNK, and Akt activation status after *TNNI3K* overexpression in NRVMs.

Fig. S6. TNNI3K-induced cell death is blunted by selective knockdown of p38 α in NRVMs.

Fig. S7. GSK854 rescues the effect of *TNNI3K* overexpression on ROS generation in NRVMs.

Fig. S8. *Tnni3k* deletion does not alter adverse LV remodeling after permanent occlusion MI.

Table S1. LV function and cardiac morphometry in inducible cardiomyocyte-specific *Tnni3k*-KO mice.

Table S2. Selectivity profiles of small-molecule TNNI3K inhibitors.

Methods

Reagents

All reagents and chemicals were purchased from Sigma-Aldrich unless otherwise noted. Primary antibodies: TNNI3K (#SAB4502101) from Sigma-Aldrich; sarcomeric α -actinin (A7811) from Sigma-Aldrich; p-p38 (#9211), p38 (#9212), p-ERK1/2 (#4377), p-JNK1/2 (#9251 and #4668), p-Akt S.473 (#4060), myc (#2276), troponin I (#4002), N-cadherin (#4061), and histone H3 (#9717) all from Cell Signaling; p38 β (PA1-41154) from Thermo Pierce, and GAPDH (#10-R-G109a) from Fitzgerald Industries Intl.

Generation of *Tnni3k* transgenic or cardiac-specific knockout mice

Cardiac-specific over-expression of TNNI3K or KI (K490R) TNNI3K was achieved via microinjection of the human TNNI3K gene downstream of the mouse α -myosin heavy chain promoter into FVB/N mice. Transgenic founder lines were then backcrossed to WT FVB/N for three generations. The TNNI3K floxed mouse was generated on the C57BL/6 background by insertion of loxP elements flanking exons 1 and 2 of the mouse *Tnni3k* gene via traditional genetic techniques. To conditionally delete *Tnni3k* in the adult heart, *Tnni3k*^{fl/fl} mice were crossed with the α -MHC-Mer-Cre-Mer (MCM) mouse, which provides cardiac-specific expression of Cre under the control of the tamoxifen-inducible modified estrogen receptor. Heterozygous MCM mice were crossed for a minimum of three generations to homozygous *Tnni3k*^{fl/fl} mice to generate *Tnni3k*^{fl/fl}/MCM^{+/-} animals. For all experiments, *Tnni3k* floxed littermates that did not express MCM served as controls (denoted as WT). At 3 months of age tamoxifen (20 mg/kg in sterile corn oil) was administered by intraperitoneal injection daily for five days. All experiments began 5 days after the last dose of tamoxifen.

Analysis of cardiac injury biomarkers

Blood was collected from the jugular vein of each animal at time of sacrifice, and plasma was isolated by centrifugation at 2000 x g for 15 minutes in anticoagulant K₂EDTA-coated tubes. Plasma was analyzed for levels of cTnI, cTnT, and MLC using the Meso Scale Discovery Cardiac Injury Panel sandwich immunoassay kit (Meso Scale Diagnostics, LLC) according to manufacturer's instructions.

Hemodynamics

For in vivo hemodynamic measurements, mice were lightly anesthetized by IP injection of tribromoethanol/amylen hydrate (Avertin; 2.5% w/v, 8 μ l/g body weight). A 1.4-French micromanometer-tipped catheter (no. SPR-671, Millar Instruments Inc.) was then inserted into the right carotid artery and advanced into the LV. Systolic blood pressure, rate of LV pressure rise (+dP/dt and -dP/dt) and heart rate were recorded in closed-chest mode, both at baseline and in response to sequential dosing of isoproterenol (0.1 – 10 ng), administered via cannulation of the right internal jugular vein.

Echocardiography

Transthoracic 2D-directed M-mode echocardiography was performed using a Vevo 770 with 12-mHz probe (Visualsonics). Mice were anesthetized by inhalation of isoflurane (1-1.5%). M-mode interrogation was performed in the parasternal short-axis view just superior to the papillary muscle. LVEDD, LVESD, and septal and LV posterior wall thicknesses were determined and used to calculate percent fractional shortening (FS) and ejection fraction (EF). FS was calculated

with the formula: $[(LVEDD-LVESD) / LVEDD] \times 100$. EF was calculated with the formula: $[(LVEDV-LVESV) / LVEDV] \times 100$ where EDV is end-diastolic volume and ESV is end-systolic volume.

Histological analysis

LV tissue was fixed overnight in 4% paraformaldehyde, dehydrated through increasing serial concentrations of ethanol, and then embedded in paraffin blocks for sectioning. Five- μm sections were cut and stained with hematoxylin and eosin (H&E) or Masson's trichrome. A Nikon Eclipse 80i microscope with NIS Elements software was used to record images. Cross-sectional area of H&E-stained cardiomyocytes was determined by an observer blinded to the conditions, with a minimum of 75 cells per heart measured for each condition. Fibrosis was measured by an observer blinded to the conditions, as percentage of trichrome-positive area, relative to total LV area, in five consecutive sections per heart.

Ex vivo cardiac superoxide detection

Cross-sections through the left ventricle (2 mm) from freshly isolated mouse hearts were prepared and then equilibrated in Krebs buffer for 30 min at 37°C. Sections were then stained with 30 μM dihydroethidium (DHE; Molecular Probes) in fresh buffer and incubated in the dark for 30 min with gentle rotation. DHE-stained LV sections were imaged using a Carl Zeiss 710 confocal microscope with a 10X dry objective at 561 nm excitation. ZEN software was used to collect sequential Z-stacked confocal line scans of each section and assemble 2.5-dimensional histogram plots of mean DHE intensity.

Cell culture and analysis

Adult mouse ventricular myocytes were isolated from 3 month-old Tg-TNNI3K, WT FVB/N, or WT C57BL/6 mice by Langendorff perfusion and enzymatic digestion. Neonatal rat ventricular myocytes (NRVMs) were isolated from 2-3 day-old Sprague-Dawley rats as previously described (Kerkela *et. al.* 2008. *J Clin Invest.* 11: 3609-18) and cultured at 37°C and 5% CO₂ in Ham's F-10 nutrient medium (F-10) with L-glutamine supplemented with 5% FBS, 100 U/mL penicillin, and 100 µg/mL streptomycin. NRVM were cultured in serum-free medium for 24 hrs prior to adenovirus infection or treatment.

Simultaneous measurement of Ca²⁺ uptake and mitochondrial membrane potential ($\Delta\Psi_m$) in permeabilized cardiomyocytes

Freshly isolated murine cardiomyocytes ($\sim 1.4 \times 10^5$), following centrifugation, were transferred to an intracellular-like medium [permeabilization buffer: 120 mM KCl, 10 mM NaCl, 1 mM KH₂PO₄, 20 mM HEPES-Tris, pH 7.2, supplemented with protease inhibitors (EDTA-free completeTM tablets, Roche Applied Science), 2 µM thapsigargin and digitonin (80 µg/ml)]. The cell suspensions were supplemented with succinate (5 mM), placed in a fluorimeter and permeabilized by gentle stirring. Fura2-FF (0.5 µM) was added at 0 s and JC-1 (800 nm) at 20 s to simultaneously measure extra-mitochondrial Ca²⁺ and $\Delta\Psi_m$. Fluorescence was monitored in a temperature-controlled (37°C) multi-wavelength-excitation dual wavelength-emission spectrofluorometer (Delta RAM, Photon Technology International) using 490/535 nm ex/em for the monomer, 570/595 nm ex/em for the J-aggregate of JC1, and 340/380 nm for Fura2-FF. Ca²⁺ pulses were added at time points indicated and CCCP was added at 765 s to determine mitochondrial Ca²⁺ content.

Mitochondrial ROS measurement

NRVMs were loaded with the mitochondrial superoxide sensitive fluorophore MitoSOX Red (Invitrogen; 10 μ M) in ECM containing 2% BSA at 37 °C for 10 min. Cells were then washed, re-suspended in ECM containing 0.25% BSA, placed on a temperature-controlled stage, and imaged using a Carl Zeiss 510 confocal microscope with a 40 x oil objective at 561 nm excitation. MitoSOX Red indicated membrane potential by fluorescing upon oxidation and binding to mitochondrial DNA (mtDNA). For experiments with additional treatments, DPI was loaded for 1 h at 3 μ M, antimycin A was loaded for 5 min at 2 μ M, ionomycin was loaded for 5 min at 2.5 μ M, and GSK854 was loaded for 1 h at 3 μ M.

Measurement of cellular oxygen consumption rate

Oxygen consumption rate (OCR) in intact NRVM was measured at 37°C in an XF96 extracellular analyzer (Seahorse Bioscience). Cells were sequentially exposed to oligomycin (1 μ M), FCCP (1.25 μ M) and rotenone (0.75 μ M) plus antimycin A (1.25 μ M) using the XF Cell Mito Stress Kit (Seahorse Bioscience), according to the manufacturer's instructions. Preliminary cell density and dose-response experiments were performed in untreated NRVMs per manufacturer's instructions to select optimal seeding density and compound concentrations.

Annexin V/PI cell death Assays

NRVM were cultured on laminin-coated, 25 mm-diameter glass coverslips and incubated with 1 μ g/mL Annexin V–Alexa Fluor Pacific Blue conjugate (Invitrogen) and 0.5 μ g/ml propidium iodide (PI; Invitrogen) for 15 minutes in Annexin V binding buffer (Invitrogen). Cells were then

imaged using a Carl Zeiss 510 confocal microscope with a 40X oil objective. Cell death was quantified as the percentage of Annexin V and PI double-positive cells over five random imaging fields per condition.

siRNA

NRVM were transfected with ON-TARGETplus pooled rat siRNAs (Thermo Pierce) against either p38 α (L-080059-02-0010), p38 β (L-110520-01-0010), or a scrambled control (AM4611). Cells were washed 2X in dPBS and then cultured in serum and antibiotic-free Opti-MEM medium for 2 h. siRNAs were delivered using Lipofectamine RNAimax (Invitrogen) according to manufacturer's instructions. All experiments were performed 48 h after siRNA transfection.

Supplementary Figures

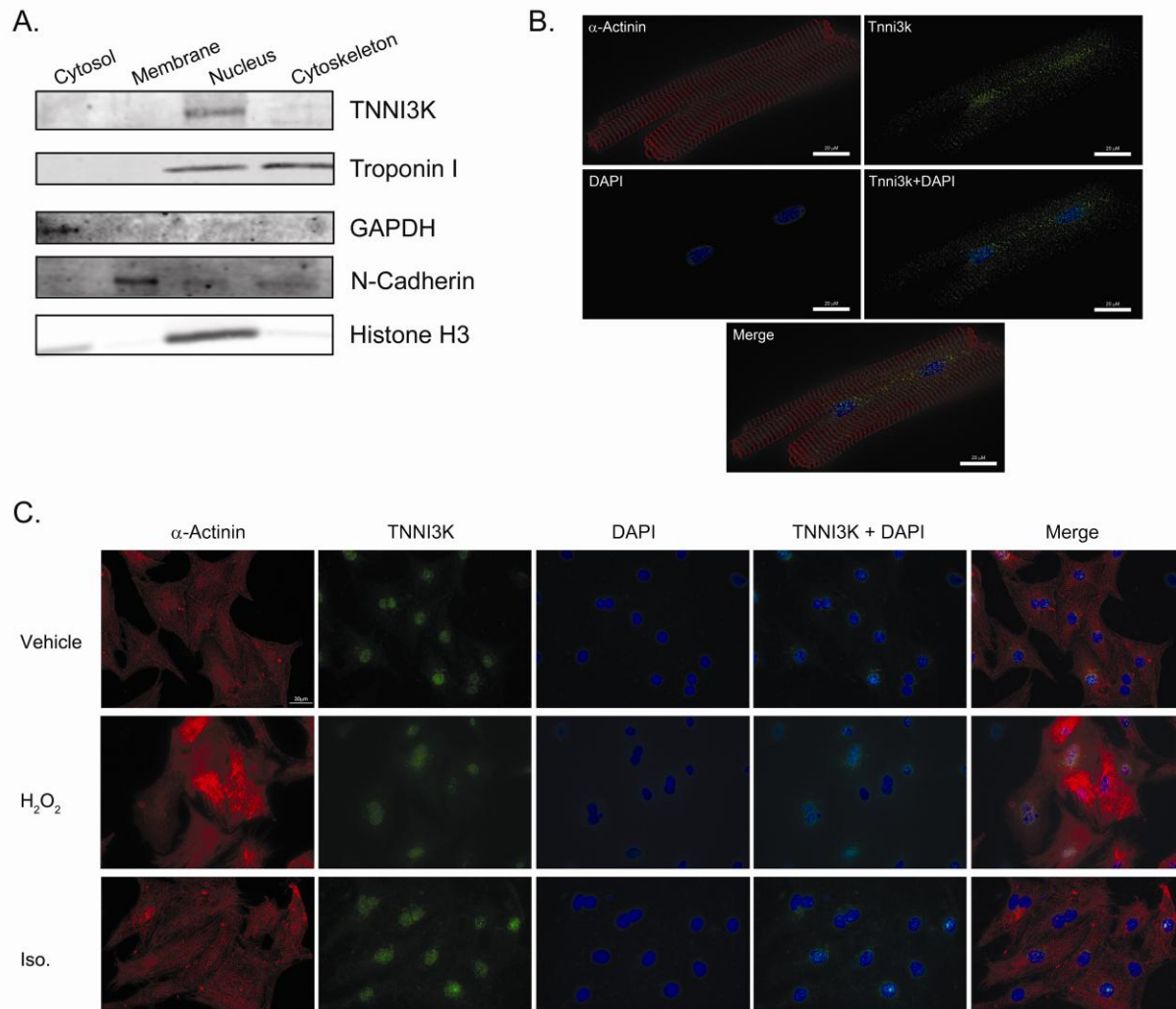


Fig. S1. TNNI3K is localized to the cardiomyocyte nucleus. (A) Analysis of TNNI3K and cTnI localization by Western blotting of subcellular fractions from isolated NRVMs. GAPDH, N-cadherin, and histone H3 served as markers of the cytosolic, membrane, and nuclear fractions, respectively. (B) Immunofluorescence micrographs of an adult rat cardiomyocyte labeled for α -actinin and TNNI3K. DAPI was used to visualize myocyte nuclei. Scale bars, 30 μ m. (C) NRVMs were treated with 100 μ M H_2O_2 , 10 μ M isoproterenol, or vehicle (dPBS) for 20 min then immunolabeled for TNNI3K and α -actinin. DAPI was used as a marker of myocyte nuclei.

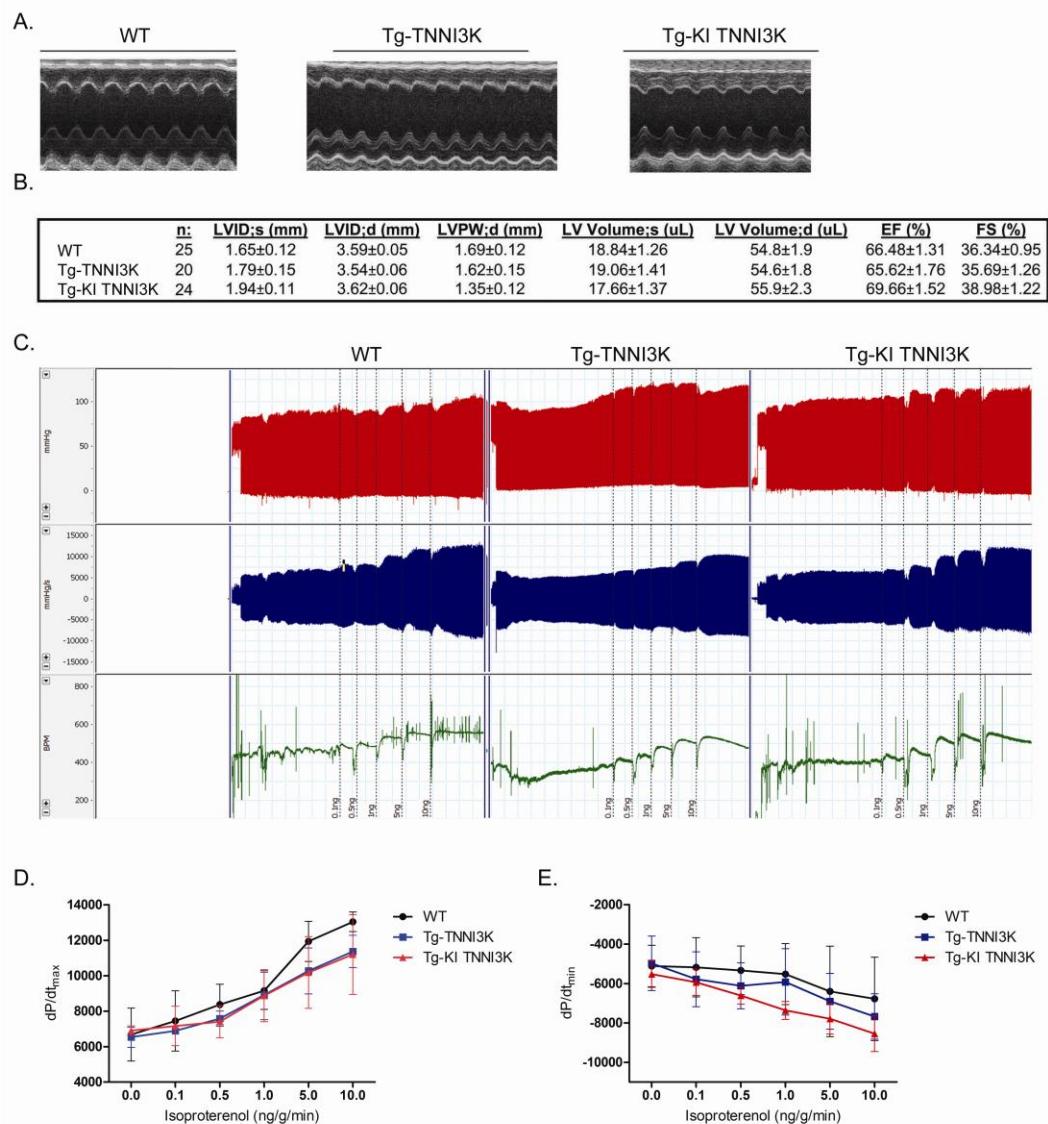


Fig. S2. Basal LV function, hemodynamics, and cardiac morphometry in Tg-TNNI3K and Tg-KI TNNI3K mice. (A) Representative M-mode echocardiograms from TNNI3K transgenic and WT mice at 3 months of age. (B) LV chamber dimensions, ejection fraction (%EF), and fractional shortening (%FS) were measured by 2D-directed M-mode echocardiography at 3 months. (C) Representative traces from $n=3$ mice per group for systolic pressure (SP), rate of LV pressure rise (+dP/dt and -dP/dt), and heart rate (HR) subjected to LV catheterization and challenged with increasing concentrations of isoproterenol. (D-E) Hemodynamic measurements of +dP/dt (D) and -dP/dt (E) in mice at baseline or in response to increasing concentrations of isoproterenol. Data are means \pm SEM from $n=3$ animals per genotype.

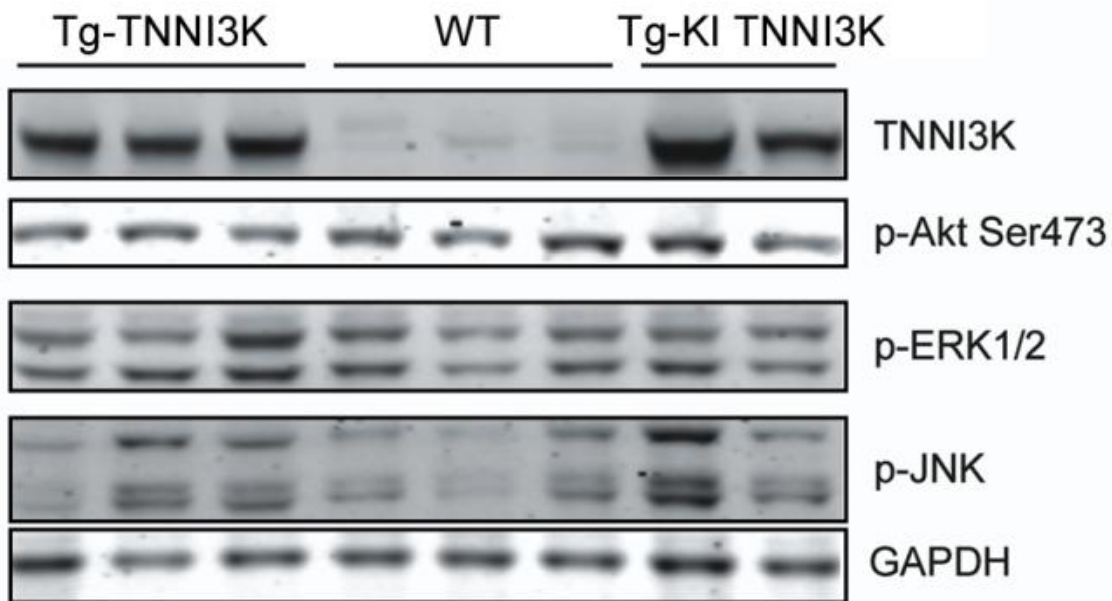


Fig. S3. Post-I/R activation status of ERK1/2, JNK, and Akt in TNNI3K transgenic mice. Continuous immunoblots for phosphorylated Akt (Ser473), ERK1/2, or JNK from the ischemic LV of mice with *TNNI3K* or KI *TNNI3K* overexpression 3 h post-I/R. GAPDH served as a loading control for total protein levels.

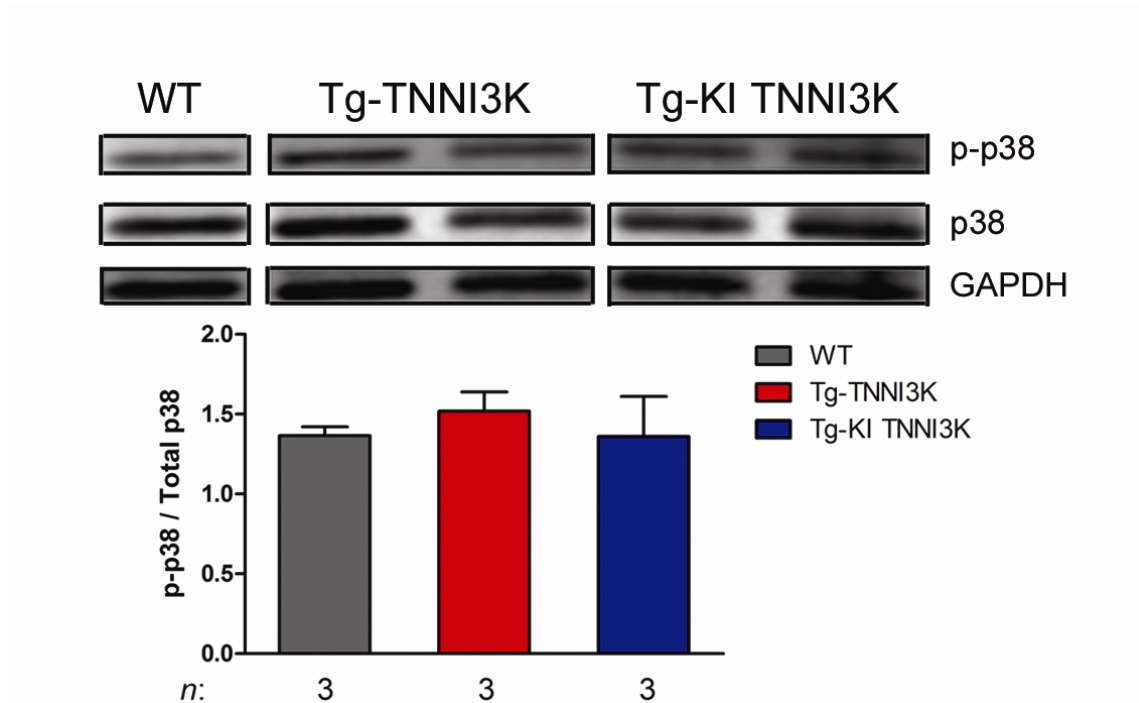


Fig. S4. Basal p38 MAPK activation status in TNNI3K transgenic mice. Representative immunoblots from $n=3$ animals per group of phosphorylated and total p38 MAPK in the LV of TNNI3K or KI TNNI3K mice. GAPDH served as a loading control for total protein levels. Quantification (as means \pm SEM) is shown below immunoblots.

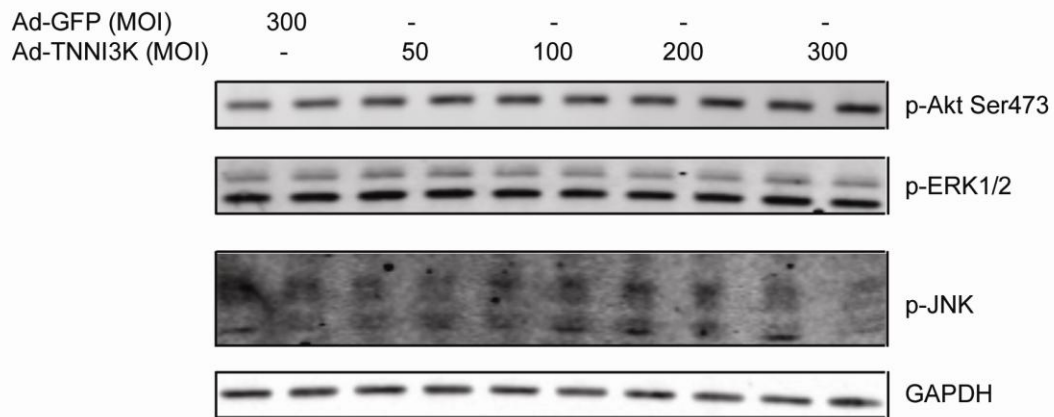


Fig. S5. ERK1/2, JNK, and Akt activation status after *TNNI3K* overexpression in NRVMs. Levels of phosphorylated Akt, ERK1/2, and JNK in samples described in Fig. 4B, from NRVMs infected with increasing MOI of adenoviruses expressing either N-terminal myc-tagged *TNNI3K* or GFP. GAPDH was used as a loading control.

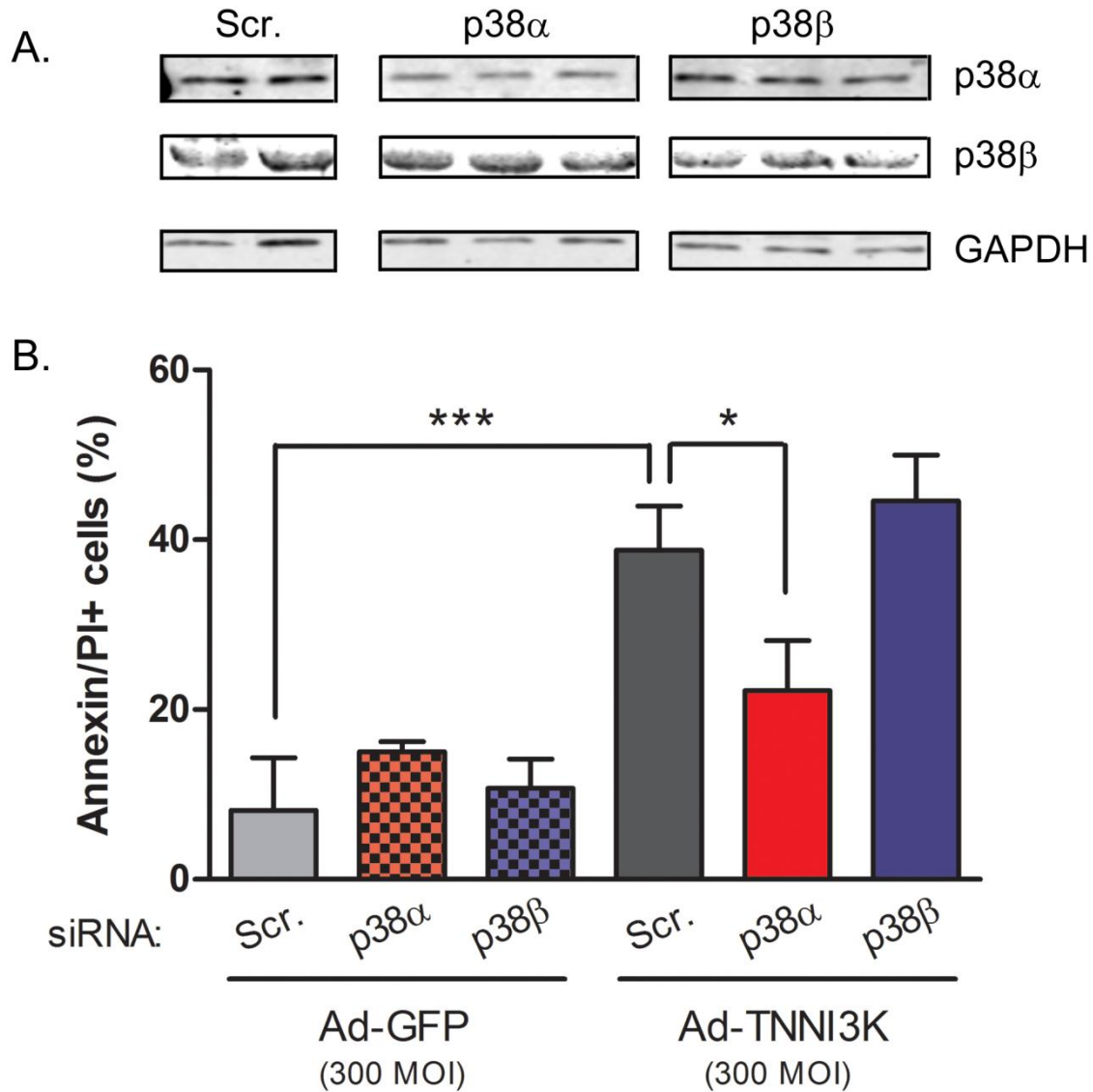


Fig. S6. TNNI3K-induced cell death is blunted by selective knockdown of p38 α in NRVMs. NRVMs were infected with adenoviruses expressing *TNNI3K* or GFP. Four hours after infection, cells were transfected with pooled siRNAs against either p38 α , p38 β , or a scrambled control. Cell death was assessed after an additional 44 h by annexin-V/PI labeling. **(A)** Selective knockdown of p38 isoforms in NRVMs as assessed by Western blot. GAPDH served as a loading control for total protein. **(B)** Quantification of cell death, as percent of annexin-V/PI double-positive cells. Data are means \pm SEM ($n=3$ biological replicates for each condition). * $P<0.05$, *** $P<0.001$, one-way ANOVA followed by Tukey's post-hoc test.

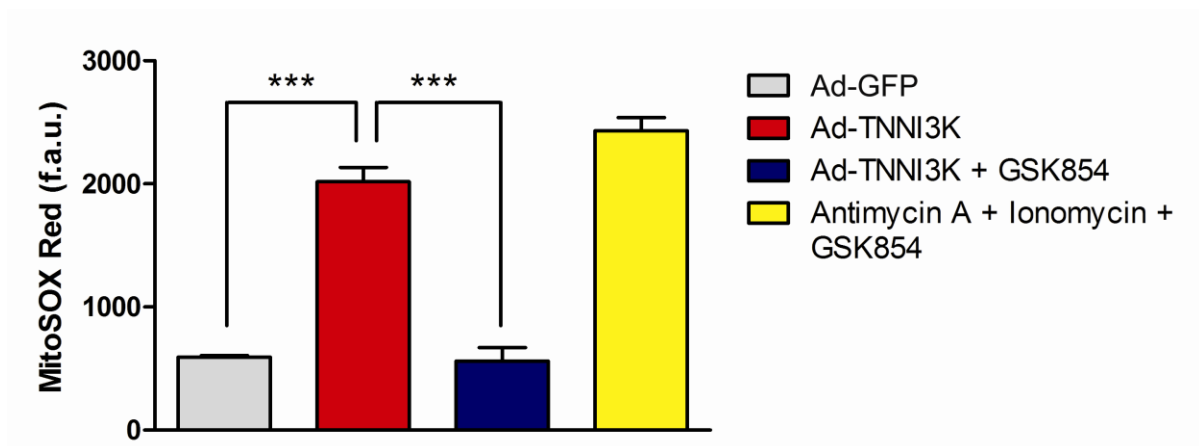


Fig. S7. GSK854 rescues the effect of *TNNI3K* overexpression on ROS generation in NRVMs. Quantification of mean MitoSOX Red fluorescence intensity in NRVMs overexpressing *TNNI3K* or GFP (control). For groups indicated, cells were treated with either GSK854 alone or with antimycin A and ionomycin, for 1 hour prior to imaging. Data are means \pm SEM from $n = 3$ biological replicates. *** $P < 0.001$, one-way ANOVA followed by Tukey's post-hoc test.

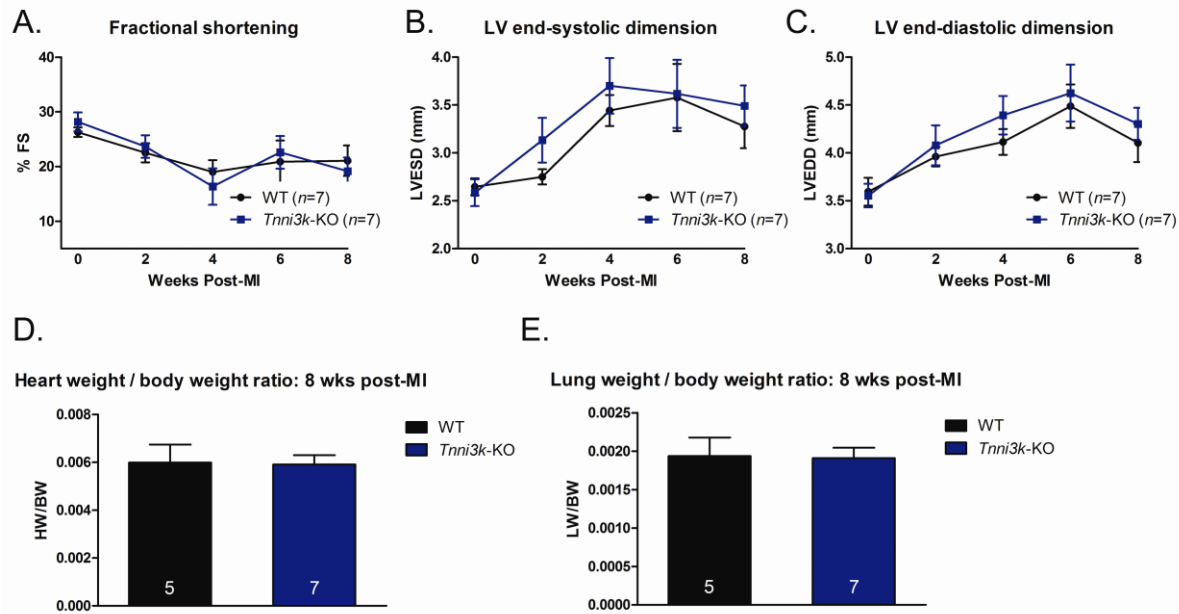


Fig. S8. *Tnni3k* deletion does not alter adverse LV remodeling after permanent occlusion MI. MI was induced via permanent LAD occlusion in *Tnni3k*-KO (Mer-Cre-Mer^{+/+}, *Tnni3k*-floxed) mice or *Tnni3k*-floxed, MCM^{-/-} littermate controls (WT). Animals were followed out to 8 weeks post-MI with serial M-mode echocardiography. (A) Fractional shortening (%FS) in the above groups post-MI. (B and C) LV end-systolic dimension (B) and LV end-diastolic dimension (C) as measured by M-mode echocardiography. (D) Heart weight-to-body weight ratios at 8 weeks post-MI. (E) Lung weight-to-body weight ratios (an indicator of congestive heart failure) at 8 weeks post-MI. All data are means \pm SEM from $n = 5-7$ animals per group, as indicated.

Table S1: LV function and cardiac morphometry in inducible cardiomyocyte-specific *Tnni3k*-KO mice. Inducible *Tnni3k* deletion in the cardiomyocyte was achieved by crossing homozygous *Tnni3k*-floxed (fl/fl) mice to a mouse expressing heterozygous (+/-) α -MHC-driven Mer-Cre-Mer (MCM). *Tnni3k^{fl/fl}*, MCM^{-/-} littermates served as controls (WT). LV chamber dimensions and LV volumes at end-systole (;s) and end-diastole (;d), % ejection fraction (EF), and % fractional shortening (FS) were assessed by M-mode echo in the animals, 5 days after completion of tamoxifen dosing. Data are means \pm SEM.

	<i>n</i>	LVID;s (mm)	LVID;d (mm)	LVPW;d (mm)	LV volume;s (μ l)	LV volume;d (μ l)	EF (%)	FS (%)
MCM ^{-/-} // <i>Tnni3k^{fl/fl}</i> (WT)	5	2.65 \pm 0.09	3.59 \pm 0.05	0.78 \pm 0.09	28.9 \pm 3.21	54.8 \pm 5.2	52.36 \pm 1.28	26.27 \pm 0.87
MCM ^{+/-} // <i>Tnni3k^{fl/fl}</i> (<i>Tnni3k</i> -KO)	7	2.58 \pm 0.14	3.55 \pm 0.12	0.91 \pm 0.07	28.35 \pm 1.87	53.42 \pm 4.38	56.87 \pm 3.19	28.17 \pm 1.75

Table S2. Selectivity profiles of small-molecule TNNI3K inhibitors. Selectivity profiles of GSK329 and GSK854. TNNI3K IC₅₀ was assessed as described in patent assay WO 2011/088027A1, available at: www.wipo.int/patentscope/search/en/WO2011088027. Selectivity was determined at two different fixed concentrations (100 nM and 1000 nM) against a panel of >180 kinases at either Millipore or Reaction Biology and is reported as percent inhibition.

Compound	TNNI3K IC₅₀ (nM)	p38α IC₅₀ (nM)	<i>n</i> kinases >50%I @ 1000 nM	<i>n</i> kinases >50%I @ 100 nM
GSK329	10	790	37	11 ^a
GSK854	6	>27,000	12	1 ^b

^aAx1, DDR2, Flt1, Flt3, Flt4, KDR, Mer, MuSK, PTK5, TAO2, TAO3. ^bZAK/MLTK.